

Investigating levels scheme of $^{226-236}\text{U}$ isotopes using interacting boson model

Ali A. Mezban^{*}  , Falih H. Al-Khudair 

Department of Physics, College of Education for Pure Sciences, University of Basrah, Basrah, Iraq.

ARTICLE INFO

Received 30 April 2025
Revised 24 May 2025
Accepted 26 May 2025
Published 30 June 2025

ABSTRACT

The nuclear structure of $^{226-236}\text{U}$ isotopes has been investigated using the interacting boson model (IBM-1). The model space is extended to include the f-boson ($L=3$) to calculate the negative parity energy levels. The ground state band (g.s.-band), beta band (β -band), gamma band (γ -band), and two negative bands have been described. The predicted wave functions have been used to calculate the transition probabilities in-band and inter-band. The nuclear shape was determined by calculating the potential energy surface (PES) as a function of deformation parameters. The model results are compared with available experimental data, and the results show good overall agreement.

Keywords :

Energy Levels, Nuclear Structure, Interacting Boson Model, Heavy Nuclei, Uranium Isotopes.

Citation: A. A. Mezban , F. H. Al-Khudair, J.Basrah Res. (Sci.) 51(1),159 (2025).
DOI:<https://doi.org/10.56714/bjrs.51.1.14>

1. Introduction

Even-even deformed nuclei are characterized by well-ordered energy bands. The fundamental evidence for the arrangement of energy levels within the structure of these bands is derived from calculations of the strength of electric quadrupole and electric dipole transitions [1]. The observation of low-lying rotational bands with $K^\pi = 0^-$ in even–even nuclei is indicative of their having strong octupole correlations. Further evidence is provided by the sizeable value of the E3 transition to the ground state [5]. Experimental studies conducted in the rare-earth area suggest stable octupole deformations at angular momentum ($J^\pi > 10^+$) [2-7]. The sequence of the negative parity band strongly depends on the Fermi level in the deformed region [8]. In heavy nuclei $A > 220$, the closely lying single particle $g_{9/2}$ and $j_{15/2}$ neutron orbitals, along with the $f_{7/2}$ and $i_{13/2}$ proton orbitals, in proximity to the Fermi level, form the basis for the existence of octupole deformation [9,10]. Theoretically, the negative levels in heavy nuclei have been studied in detail using nuclear models [11-15]. The aim of the present work is to carry out a systematic interacting boson model calculations of the even -even U-isotopes with $A = 226-236$. Special attention will focus on identifying the negative parity bands generated by adding an f-boson to the model space. As well as to investigate the potential energy surface of the studied nuclei.

*Corresponding author email: pgs.ali.abdalkareem@uobasrah.edu.iq



©2022 College of Education for Pure Science, University of Basrah. This is an Open Access Article Under the CC by License the [CC BY 4.0](#) license.

N: 1817-2695 (Print); 2411-524X (Online)
line at: <https://jou.jobrs.edu.iq>

2. Interacting Boson Model

Arima and Iachello proposed the Interacting Boson Model (IBM) of nuclear structure, which has been widely used to study the nuclear structure of even-even nuclei [16-20]. The main aim of the model is to calculate the energy levels, so it is necessary to write the Hamiltonian of the system. In the sd-space, with creation ($s^\dagger d^\dagger$) and annihilation (sd) operators for $s(L = 0)$ and $d(L = 2)$ bosons, respectively. The general form in one body and two body terms is written [16-18].

$$\begin{aligned}
H = E_0 + \varepsilon_s(s^\dagger, \tilde{s}) + \varepsilon_d \Sigma_\mu d^\dagger_\mu, \tilde{d}_\mu + \sum_{L=0,2,4} \frac{1}{2} (2L+1)^{1/2} C_L \left[(d^\dagger \times d^\dagger)^L \times (\tilde{d} \times \tilde{d})^L \right]_0^{(0)} \\
+ \frac{1}{\sqrt{2}} \nu_2 [(d^\dagger \times d^\dagger)^{(2)} \times (\tilde{d} \times \tilde{s})^{(2)} + (d^\dagger \times s^\dagger)^{(2)} \times (\tilde{d} \times \tilde{d})^{(2)}]_0^{(0)} \\
+ \frac{1}{2} \nu_0 [(d^\dagger \times d^\dagger)^{(0)} \times (\tilde{s} \times \tilde{s})^{(0)} + (s^\dagger \times s^\dagger)^{(0)} \times (\tilde{d} \times \tilde{d})^{(0)}]_0^{(0)} \\
+ u_2 \left[(d^\dagger \times s^\dagger)^{(2)} \times (\tilde{d} \times \tilde{s})^{(2)} \right]_0^{(0)} \\
+ \frac{1}{2} u_o \left[(s^\dagger \times s^\dagger)^{(0)} \times (\tilde{s} \times \tilde{s})^{(0)} \right]_0^{(0)}. \tag{1}
\end{aligned}$$

Where $C_L (L = 0,2,4)$, $u_L (L = 0,2)$ and $\nu_L (L = 0,2)$ represent the two body interaction parameters. The Hamiltonian operator can also be expressed in terms of a boson-boson multipole interaction and takes the following form [19]:

$$\hat{H}_{sd} = \varepsilon_d n_d + a_0 \hat{P} \cdot \hat{P} + a_1 \hat{L} \cdot \hat{L} + a_2 \hat{Q} \cdot \hat{Q} + a_3 \hat{T}_3 \cdot \hat{T}_3 + a_4 \hat{T}_4 \cdot \hat{T}_4 \tag{2}$$

where ε_d is the boson energy; $a_i (i = 0 - 4)$ represent the strengths of the pairing, angular momentum, quadrupole, octupole and hexadecupole interactions between the bosons, respectively. The strength of these interactions in the Hamiltonian depends on the nucleus's shape. In particular, the level scheme of SU(3) nuclei corresponds to the values of the a_1 and a_2 parameters.

Extending the model space to include the f ($L = 3$) boson, the system's Hamiltonian is written as follows [20-23]:

$$H = H_{sd} + H_f + V_{sdf}. \tag{3}$$

H_{sd} the Hamiltonian in sd -space interaction as in Eq. (2). $H_f = E_f n_f$. where n_f and E_f are the number of f -boson operator and their energy. V_{sdf} describes boson's interaction in sdf -space. The multipole expansion has been used in the form

$$V_{sdf}^{Mult} = A_1 L_d \cdot L_f + A_2 Q_d \cdot Q_f - A_3 Q^3 \cdot Q^3. \tag{4}$$

$$L_d \cdot L_f = -2\sqrt{210} [(d^\dagger \tilde{d})^{(1)} \times (f^\dagger \tilde{f})^{(1)}]_0^{(0)} \tag{5}$$

$$Q_d \cdot Q_f = -2\sqrt{35} [((d^\dagger \tilde{s}) + (s^\dagger \tilde{d}))^{(2)} - \chi(d^\dagger \tilde{d})^{(2)} \times (f^\dagger \tilde{f})^{(2)}]_0^{(0)} \tag{6}$$

$$Q^3 = (s^\dagger \tilde{f} + f^\dagger \tilde{s})^{(3)} - \chi_3(d^\dagger \tilde{f} + f^\dagger \tilde{d})^{(3)} \tag{7}$$

The electric transition operator $T^{(EL)}$ $L = 1, 2, 3$ in the IBM has the following form

$$T^{E1} = e_{1Q} [T^{E2} \times (s^\dagger \tilde{f} + f^\dagger \tilde{s})^{(3)}]^{(1)} + e_{1df} (d^\dagger \tilde{f} + f^\dagger \tilde{d})^{(1)} \tag{8}$$

$$T^{E2} = e_{2sd} (d^\dagger \tilde{s} + s^\dagger \tilde{d})^{(2)} + e_{2dd} (d^\dagger \tilde{d})^{(2)} \tag{9}$$

$$T^{E3} = e_{3Q}[T^{E2} \times (s^\dagger \tilde{f} + f^\dagger \tilde{s})^{(3)}]^{(3)} + e_{3sf}(s^\dagger \tilde{f} + f^\dagger \tilde{s})^{(3)} + e_{3df}(d^\dagger \tilde{f} + f^\dagger \tilde{d})^{(3)} \quad (10)$$

The PES can be thoroughly described to clarify the fundamental ideas of nuclear structure. The PES formal is used as a function of the deformation parameters β and γ [17,24]

$$V(\beta, \gamma) = \frac{N_B}{1 + \beta^2} (R_1 + R_2 \beta^2) + \frac{N_B(N_B - 1)}{(1 + \beta^2)^2} (R_3 \beta^4 + R_4 \beta^3 \cos 3\gamma + R_5 \beta^2 + R_6) \quad (12)$$

where R_i is related to the model Hamiltonian in sd -space parameters [20]. N_B is boson number.

3. Energy Levels

To calculate the energy levels of $^{226-236}\text{U}$ isotopes, the Hamiltonian in Eq. (3) has been diagonalized by PHINT code [26]. The proton and neutron boson numbers have been determined, corresponding to $Z=82$ and $N=126$ closed shells. The energy ratio $R_{4/2} = E4_1^+ / E2_1^+$ has been calculated as shown in Table 1. These values indicate that these isotopes belong to the rotational limit. The values of the parameters are chosen to fit the experimental data as shown in Table 2.

Table 1. The value of the energy ratio $R_{4/2} = E4_1^+ / E2_1^+$ of $^{226-236}\text{U}$

A	EXP	IBM
226	3.08	3.32
228		3.40
230	3.31	3.37
232	3.31	3.37
234	3.32	3.38
236	3.31	3.38

Table 2. The values of the parameters of the Hamiltonian used in Eq. (3). $\chi = -1.322$ for all isotopes

A	N _B	a ₁	a ₂	A ₁	A ₂	A ₃
226	9	-0.0200	0.005	-0.01	-0.024	0.01
228	10	-0.0110	0.005	-0.01	-0.01	0.01
230	11	-0.0110	0.004	-0.001	-0.001	0.01
232	12	-0.0110	0.004	-0.026	-0.01	0.02
234	13	-0.0110	0.003	-0.03	-0.01	0.01
236	14	-0.0120	0.003	-0.021	-0.01	0.01

3.1. Levels scheme of the ^{226}U isotope

This isotope has 92 protons and 134 neutrons with 5 proton bosons and 4 neutron bosons. The total number of bosons is 9, and according to the theoretical foundations of the model, the maximum angular momentum that can be calculated is $J = 2N = 18$. The model calculations for the low-lying levels of the ^{226}U isotope show a trend close to the SU(3) as shown in Fig. 1. Three positive parity energy bands and two negative parity bands have been plotted. Experimentally [27], the energy of the $J^\pi = 2_1^+ - 14_1^+$ for ground state band have been observed. The energy of $J^\pi = 6_1^+$ is equal to

0.524 MeV and 0.483 MeV in the model and experimental results, respectively. For the other levels, the difference increases significantly with increasing angular momentum. For β and γ bands levels, no experimental data have been observed yet. Theoretically, the energies of these bands head are equal $E(J^\pi = 0_2^+) = 1.019$ MeV and $E(J^\pi = 2_2^+) = 1.0944$ MeV. Regarding negative parity states, the figure included two bands. The states of the first one are $J^\pi = 1^-, 3^-, 5^-, 7^-, 9^-, 11^-, 13^-$. A comparison of the calculated values with available observed values shows a good agreement, and the sequence has been achieved. The theoretical energy of the $J^\pi = 5^-, 7^-, 9^-$ states are 0.404, 0.653, and 0.998 MeV, while the empirical values are equal to 0.447, 0.669, and 0.950 MeV, respectively. For the second band, there are no empirical values and the calculated energy of the first state the $J^\pi = 2_1^-$ equal to 0.356 MeV.

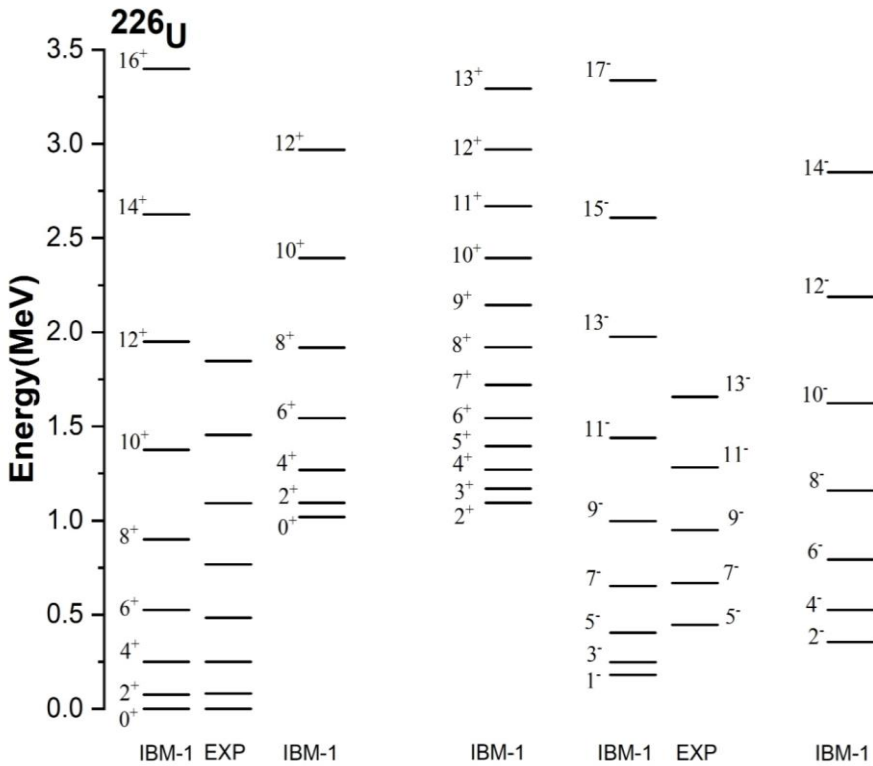


Fig.1. Theoretical and available experimental [27] energy levels for ^{226}U isotope

3.2. Levels scheme of the ^{228}U isotope

With a total number of bosons equal to 10, the level scheme of ^{228}U has been plotted in Figure 2. Experimentally, only $E(2_1^+)$ has been observed yet. The energy of this state is equal to 0.059 MeV and 0.054 MeV in the model and experimental results, respectively. The members of the ground state band appear up to the $J^\pi = 18_1^+$ in the figure with 3.120 MeV. For β - band, the energy of the $J^\pi = 0_2^+$ is equal to 0.681 MeV while the energy of the $J^\pi = 16_2^+$ is equal to 3.108 MeV. On the other hand, the $E(2_2^+) = 0.682$ MeV. The predicted energies of the negative-parity states $1_1^- (K^\pi = 1^-)$ and $2_1^- (K^\pi = 2^-)$ are equal to 0.278 MeV and 0.347 MeV, respectively.

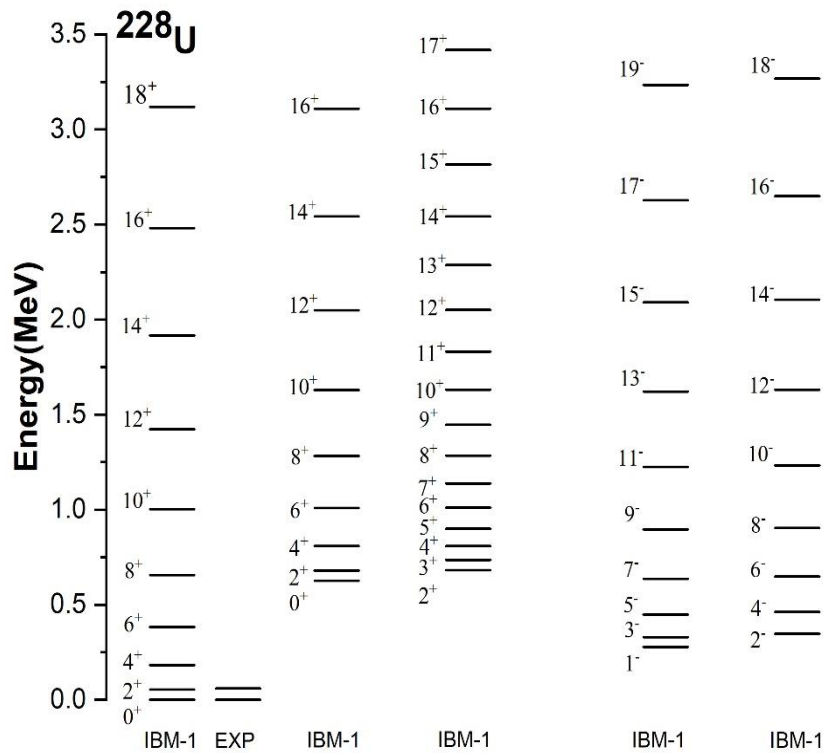


Fig. 2. Theoretical and available experimental [27] energy levels for the ^{228}U isotope.

3.3. Levels scheme of the ^{230}U isotope

The theoretical and available experimental data have been plotted in Figure 3. One can see that the model predicts very well the energies of ground state band members. For example, the energy of $J^\pi = 2_1^+ - 10_1^+$ are equal to 0.049, 0.162, 0.341, 0.585, and 0.894 MeV in the model calculation compared with the observed ones of 0.051, 0.169, 0.346, 0.578, and 0.856 MeV. The 2_3^+ , 3_1^+ , and 4_3^+ states have similar behaviors, and these levels are members of the γ -band. At the best fit, their calculated energies are equal to 0.741, 0.790, and 0.855 MeV, respectively. We conclude that the 0_2^+ state lies below the 2_2^+ state, so it shows the appearance of a β -band below the γ -band. According to this study, the 1_1^- state appears at 0.399 MeV and 0.366 MeV in the model and observed results, respectively. Our calculated first 9^- states at 0.957 MeV are close to the observed one at 0.958 MeV. The 2_1^- ($k^\pi = 2^-$) state is the band head that appears in the model calculation at 0.340 MeV.

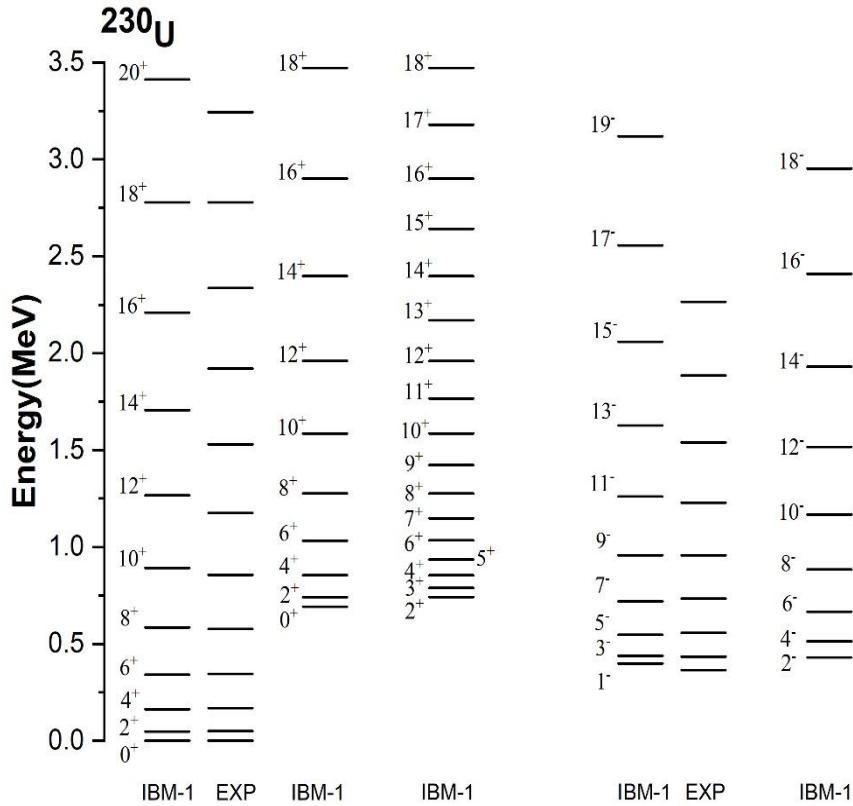


Fig. 3. Theoretical and available experimental [22] energy levels for the ^{230}U isotope.

3.4. Levels scheme of the ^{232}U isotope

As seen in figure 4, the model results are compared with the available experimental values for the five bands. The theoretical results and the experimental data of the ground-band levels showed agreement up to $J^+ \leq 10^+$ levels. Concerning the β -band, the calculated and experimental energies of the $(0_2^+, 2_2^+)$ levels are $(0.758, 0.807 \text{ MeV})$ and $(0.691, 0.734 \text{ MeV})$, respectively. For the γ -band, the third 2^+ level (band head) is predicted at 0.808 MeV , which is the observed one at 0.866 MeV . The second level in this band $J^\pi = 3_1^+$ appears at 0.911 and 0.857 MeV in the experimental and model results. From the figure, one can see that a good agreement exists between the calculated and experimental data for the first negative band. For example, the energies of the $(1^-, 3^-)$ states are equal to $(0.563, 0.628 \text{ MeV})$ experimental and $(0.584, 0.617 \text{ MeV})$ theoretical, respectively. On the other hand, it can be noted that the levels of the second negative band are not the f-boson states, where the energy of the lowest level ($J^\pi = 2^-$) is equal to 1.016 and 0.528 MeV experimentally and theoretically, respectively. maybe they are p-boson ($L=1$) levels.

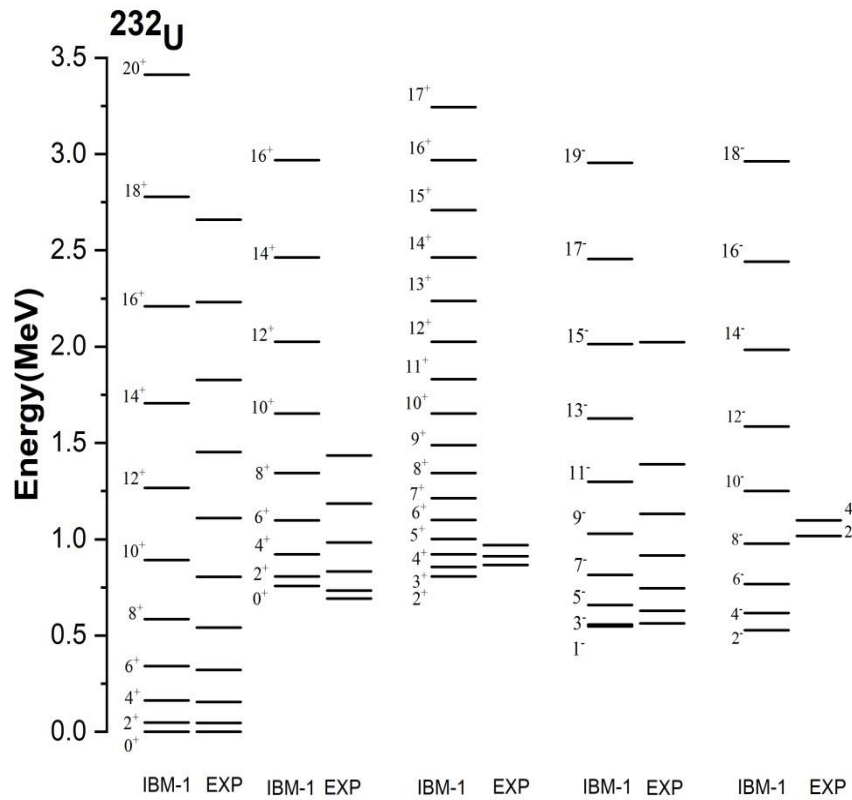


Fig. 4. Theoretical and available experimental [27] energy levels for the ^{232}U isotope.

3.5. Levels scheme of the ^{234}U isotope

In this case, there are thirteen bosons. The comparison between the calculated and available experimental data has been shown in figure (5). The main advantage of the energy scheme is that all available experimental states have been produced well. For instance, the observed energy 10_1^+ is equal to 0.7142 MeV compared to the theoretical value of 0.7837 MeV. The calculated energies of the $J^\pi = 0_2^+, 2_2^+, 4_2^+, 6_2^+$ and 8_2^+ states that the members of the β -band are equal to 0.824, 0.867, 0.967, 1.123 and 1.337 MeV, while the experimental ones are equal to 0.809, 0.851, 0.947, 1.096 and 1.292 MeV, respectively. For the γ -band, the model calculations are consistent with observed data, as shown in the figure. This first negative band is characterized by a high approach of the values to the $J^\pi = 11^-$ level. This indicates that observed and theoretical values demonstrate these approaches throughout the levels. For example, the experimental energies of the $J^\pi = 3^-$ and 5^- levels are equal to 0.628 and 0.746 MeV, while their theoretical values are 0.731 and 0.855 MeV. The behavior of the second negative band level is similar to that of the other isotopes. The figure illustrates the discrepancy between the calculated values and the available experimental values.

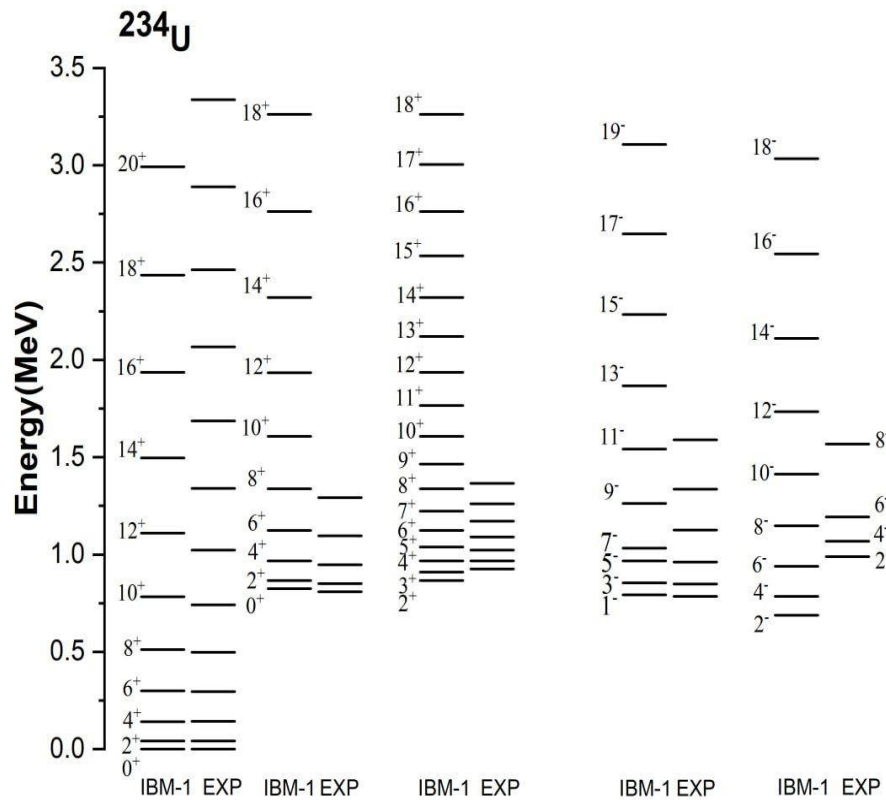


Fig. 5. Theoretical and available experimental [27] energy levels for the ^{234}U isotope.

3.6. Levels scheme of the ^{236}U isotope

A comparison between the results of the IBM-1 model and the available data for each of the five band members has been shown in figure 6. The calculated excitation energies are obtained by diagonalizing the Hamiltonian with a system of the 14 bosons. The theoretical energy values for the low-lying of the ground band show a great deal of convergence and a slight difference in the observed energy from ($J^\pi = 6^+ - 10^+$) levels. As for the β and γ bands, the observed ones are lower than the theoretical ones, and the sequence has been archived. Up to the energy range of 3.5 MeV, the energy of the first negative band levels up to ($J^\pi = 19^-$) level was obtained. The figure shows consistency between the theoretical and practical values, especially for ($J^\pi \leq 11^-$) levels. Similar to previous isotopes, the calculated energy values for the second negative band levels were found to be far from the experimental values. This difference indicates that these levels are outside the used model space.

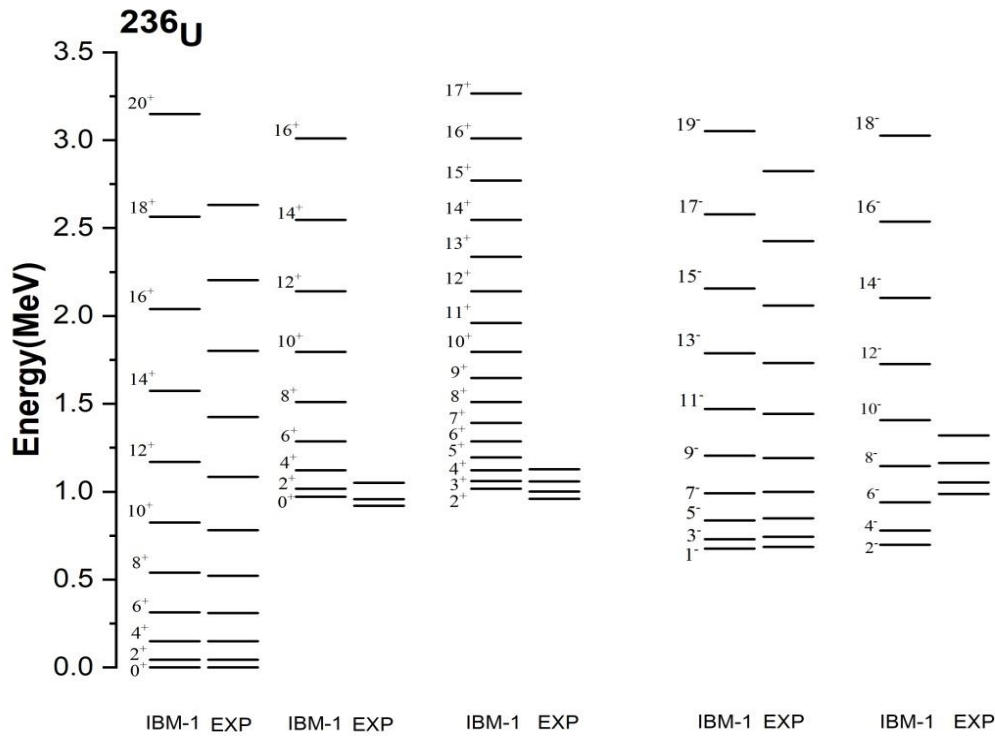


Fig. 6. Theoretical and available experimental [27] energy levels for the ^{236}U isotope.

4. Electric Transition Probabilities

The operator in Eq. (9) was used to calculate the quadrupole transition probability $B(E2)$. The α_2 and β_2 parameters have been chosen to fit the experimental value of the $(E2; 2_1^+ \rightarrow 0_1^+)$ and SU(3) limit properties. The $\alpha_2 = 0.200, 0.205, 0.2157, 0.2260, 0.2247$, and 0.2330 eb have been used for $^{226-236}\text{U}$ isotopes, respectively. The value of these parameters reflects the deformed rotational limit [12]. The $B(E2)$ values have been listed in Table 3. The experimental results were taken from Ref. [27]. For all isotopes, the transitions between members of the ground band were found to have the greatest $B(E2)$ value. From the table, one can see the a good agreement between the calculated and experimental data for the ^{236}U isotope. For the $B(E1)$ calculation, The $e_{1Q} = 0.0005 e b^{1/2}$ and $e_{1df} = 0.0025 e b^{1/2}$ for all isotopes. To estimate the values of e_{3Q} and e_{3sf} in the E3 operator, the observed $B(E3; 3_1^- \rightarrow 0_1^+)$ values in the $^{234,236}\text{U}$ isotopes have been fitted. For all isotopes, the $e_{3sf} = 0.3 e b^{3/2}$, and $e_{3Q} = 0.5, 0.45, 0.55, 0.55, 0.55$, and $0.3 e b^{3/2}$. The $B(E1)$ and $B(E3)$ values have been listed in Tables 4 and 5. To check the value of the transition probability regarding the dynamical symmetry of the model, the $B(E2)$ ratios for several transitions have been calculated. Table 6 displays the ratio values with an IBM limit [28]. It is evident that the values reflect the SU(3) limit properties.

Table 3. Theoretical $B(E2)$ values for $^{226-230}\text{U}$ isotopes in $(e^2 b^2)$ unit. Available observed data [27] is provided in the second row.

$J_i^+ \rightarrow J_f^+$	^{226}U	^{228}U	^{230}U	^{232}U	^{234}U	^{236}U
$2_1 \rightarrow 0_1$	1.6011	1.6821	1.8623 1.8621(2265)	2.0444 2.0450(1782)	2.0209 2.0256(858)	2.1730 2.1529(694)
$4_1 \rightarrow 2_1$	2.2609	2.3753	2.6298	2.8869	2.8538	3.0685 2.9516(2083)

6₁ → 4₁	2.4379	2.5613	2.8357	3.1129	3.0772	3.1129
8₁ → 6₁	2.4730	2.5982	2.8765	3.1578	3.1215	3.3422(1823)
10₁ → 8₁	2.4340	2.5572	2.8311	3.1079	3.0723	3.3564
2₂ → 0₂	0.0117	0.0124	0.0136	0.0150	0.0148	3.3856(347)
2₂ → 2₁	0.1216	0.1277	0.1414	0.1553	0.1535	0.1650
2₃ → 2₁	0.0193	0.0203	0.0224	0.0246	0.0243	0.0262
2₃ → 2₂	0.0125	0.0129	0.0145	0.0159	0.0157	0.0421(69)
4₂ → 2₂	0.8309	0.8731	0.9665	1.0610	1.0488	0.0159
3₁ → 2₁	0.1365	0.1434	0.1588	0.1743	0.1723	1.1277
3₂ → 2₂	0.0191	0.0200	0.0222	0.0244	0.0241	0.1853
3₁ → 4₁	0.0693	0.0728	0.0806	0.0880	0.0875	0.0259
5₁ → 3₁	1.3135	1.3800	1.5278	1.6772	1.6579	0.0941
5₁ → 4₁	0.1095	0.1151	0.1274	0.1399	0.1383	1.7827
						0.1487

Table 4. IBM B(E1) and B(E3) in $e^2 b$ and $e^2 b^3$ unit, respectively, for $^{226-230}\text{U}$ isotopes.

Transition	^{226}U		^{228}U		^{230}U		
	$J_i^- \rightarrow J_f^+$	B(E1)	B(E3)	B(E1)	B(E3)	B(E1)	B(E3)
1 ₁ → 0 ₁	2.8×10^{-4}			4.4×10^{-4}		6.1×10^{-4}	
1 ₁ → 2 ₁	1.4×10^{-4}	0.50423		9.3×10^{-5}	0.53070	3.4×10^{-4}	1.5399
1 ₁ → 4 ₁		0.22614			0.12094		0.09606
3 ₁ → 0 ₁		0.18951			0.16030		0.12983
3 ₁ → 2 ₁	3.7×10^{-4}	0.25517		4.9×10^{-4}	0.24916	5.2×10^{-4}	1.1141
3 ₁ → 4 ₁	4.4×10^{-5}	0.19498		2.1×10^{-5}	0.19241	2×10^{-5}	0.33130
2 ₁ → 2 ₁	2.9×10^{-4}	0.05152		3.7×10^{-4}	0.02852	2.2×10^{-4}	0.00099
2 ₁ → 4 ₁		0.20736			0.23469		0.64405
5 ₁ → 4 ₁	3.8×10^{-5}	0.25190		4.8×10^{-4}	0.26320	5.1×10^{-4}	1.2704
5 ₁ → 2 ₁		0.23374			0.19215		0.25549
4 ₁ → 2 ₁		0.00312			0.00156		0.93311
4 ₁ → 4 ₁	2.7×10^{-4}	0.08679		3.2×10^{-4}	0.06914	1.7×10^{-4}	1.0637
7 ₁ → 4 ₁		0.17942			0.15119		0.26379
7 ₁ → 6 ₁	3.6×10^{-4}	0.26906		4.6×10^{-4}	0.29118	4.9×10^{-4}	1.2378

Table 5. IBM B(E1) and B(E3) in $e^2 b$ and $e^2 b^3$ unit, respectively for $^{232-236}\text{U}$ isotopes.

Available observed data [27] is provided in the second row.

Transition	^{232}U		^{234}U		^{236}U		
	$J_i^- \rightarrow J_f^+$	B(E1)	B(E3)	B(E1)	B(E3)	B(E1)	B(E3)
1 ₁ → 0 ₁	2.08×10^{-4}			5.6×10^{-4}		8.8×10^{-4}	
1 ₁ → 2 ₁	4.1×10^{-4}	0.19125		1.9×10^{-4}	0.88245	9.2×10^{-5}	0.06451
1 ₁ → 4 ₁		0.78718			0.38755		0.07884
3 ₁ → 0 ₁		0.11020			0.09373		0.07962
					0.0928(57)		0.07571(1)
3 ₁ → 2 ₁	2.9×10^{-4}	0.07322		3×10^{-6}	0.00005	6.9×10^{-4}	0.01653
3 ₁ → 4 ₁	1.7×10^{-4}	0.38006		3×10^{-6}	0.39577	2.7×10^{-5}	0.08428
2 ₁ → 2 ₁	6.5×10^{-5}	0.54012		1×10^{-6}	0.35926	2.5×10^{-4}	0.22190

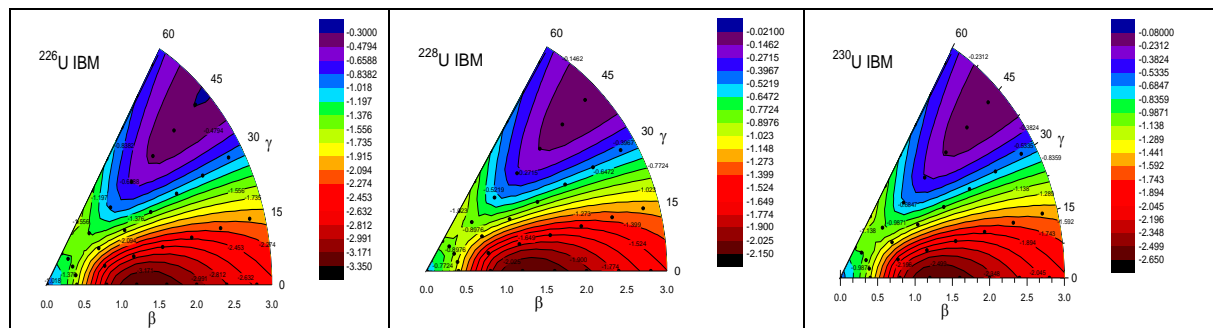
$2_1 \rightarrow 4_1$		0.01007		0.19302		0.00896
$5_1 \rightarrow 4_1$	1.8×10^{-5}	0.02506	1.3×10^{-5}	0.03156	8.4×10^{-4}	0.00012
$5_1 \rightarrow 2_1$		0.06752		0.04673		0.06303
$4_1 \rightarrow 2_1$		0.07073		0.12070		0.10304
$4_1 \rightarrow 4_1$	1.2×10^{-4}	0.59208	4×10^{-6}	0.10547	3.6×10^{-4}	0.17761
$7_1 \rightarrow 4_1$		0.03475		0.01112		0.03932
$7_1 \rightarrow 6_1$	1×10^{-5}	0.01490	4×10^{-5}	0.07571	8.9×10^{-5}	0.00048

Table 6. Calculated B(B(E2) ratios and IBM limit [28] in U isotopes.

Ratio	^{226}U	^{228}U	^{230}U	^{232}U	^{234}U	^{236}U	U(5)	SU(3)	O(6)
$R_1 = \frac{2_2^+ \rightarrow 0_1^+}{2_2^+ \rightarrow 2_1^+}$	0.640	0.640	0.640	0.640	0.640	0.640	0.011	0.70	0.070
$R_2 = \frac{2_2^+ \rightarrow 2_1^+}{2_1^+ \rightarrow 0_1^+}$	0.075	0.075	0.075	0.075	0.075	0.075	1.40	0.02	0.79
$R_3 = \frac{4_1^+ \rightarrow 2_1^+}{2_2^+ \rightarrow 2_1^+}$	18.59	18.60	18.59	18.58	18.59	18.59	1.0	6.93	1.84
$R_4 = \frac{3_1^+ \rightarrow 2_1^+}{3_1^+ \rightarrow 4_1^+}$	1.969	1.969	1.970	1.980	1.969	1.969	0.06	2.50	0.12

5. Potential energy surface

The potential energy surface $V(\beta, \gamma)$ for uranium nuclei as a function of the deformation parameters β and γ is represented in Figure 7. The β deformation parameter in Eq. (12) is arranged by the distortion factor to the Bohr Collective Model (BCM) as $\beta_{IBM} \cong \frac{A}{2.36N_B} \beta_{BCM}$, where A is the mass number [29]. It appears that all nuclei are deformed shapes with minimum values at $\beta = 1.2\text{-}1.4$ and $\gamma = 0^\circ$. In order to investigate the nuclear shape, we calculate PES as a function of $\beta = 0\text{-}3$ for $\gamma=0^\circ, 30^\circ$, and 60° as shown in Figure 8. Clearly, the $V_{min}(\beta, \gamma)$ value is on the curve of $\gamma=0^\circ$, and it was as follows: $V_{min}(\beta, \gamma) = V_{min}(1.4, 0^\circ) = -3.3426$, $V_{min}(1.2, 0^\circ) = -2.1497$, $V_{min}(1.2, 0^\circ) = -2.6388$, $V_{min}(1.4, 0^\circ) = -3.1885$, $V_{min}(1.4, 0^\circ) = -3.7369$, and $V_{min}(1.4, 0^\circ) = -4.7976$ MeV for $^{226}\text{-}^{236}\text{U}$ isotopes, respectively. The V_{min} values and deformation parameters align with the rotational limit SU (3), primarily exhibiting a prolate shape.



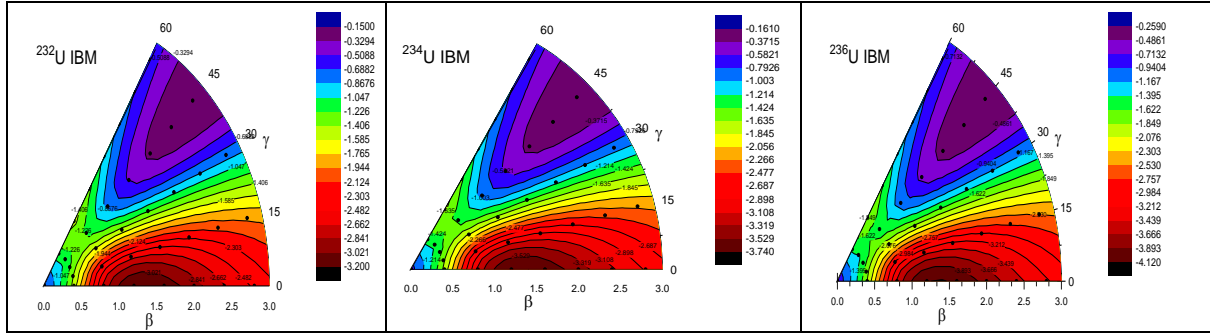


Fig. 7. The IBM potential energy surfaces for the considered $^{226-236}\text{U}$ isotopes, within deformation parameters: $0^0 \leq \gamma \leq 60^0$ and $0 \leq \beta_2 \leq 3$.

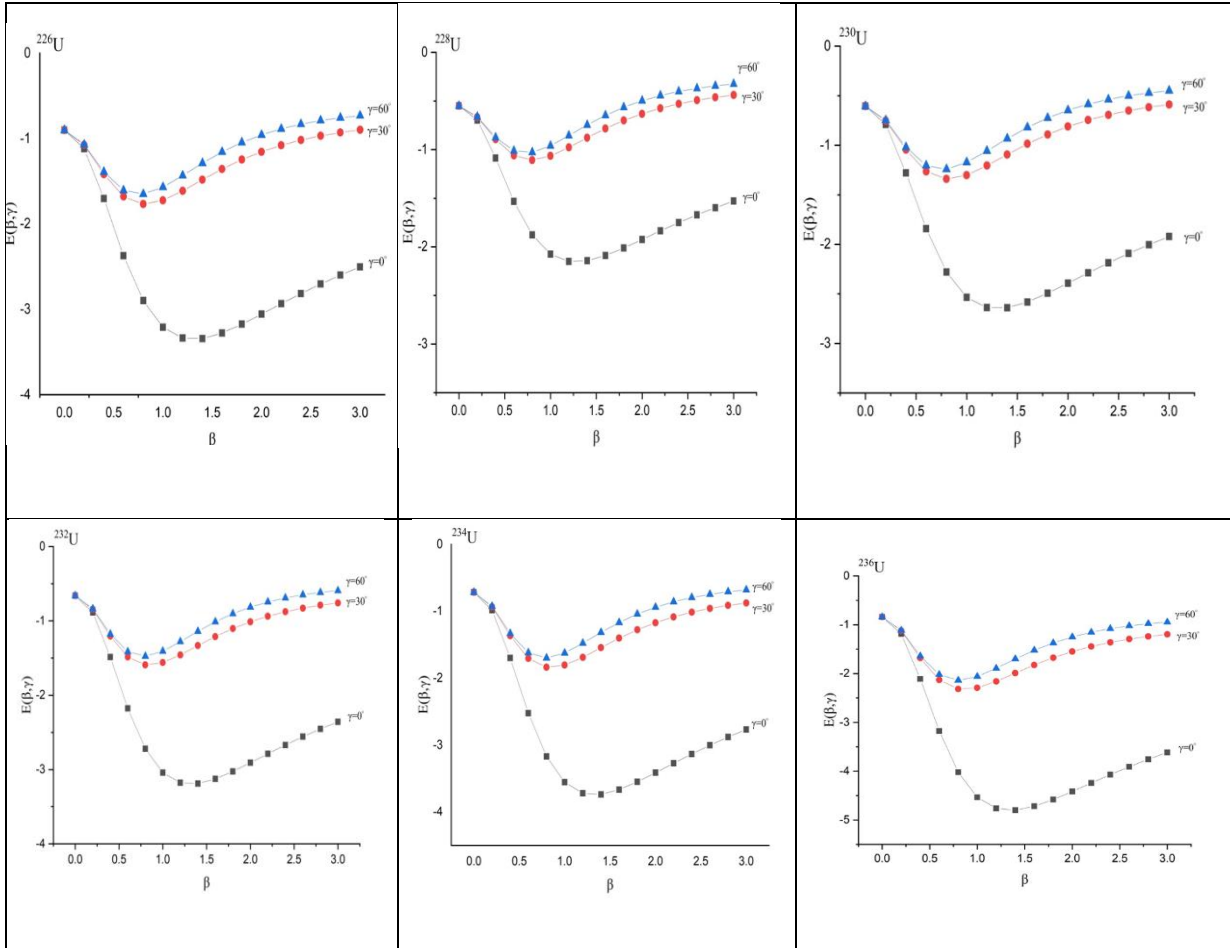


Fig. 8. The potential energy surfaces values as a function of $0 \leq \beta \leq 3$ and $\gamma = 0^0, 30^0$, and 60^0 for the $^{226-236}\text{U}$ isotopes.

6. Conclusion

The nuclear structures of even-even uranium isotopes ($A=226-236$) have been investigated using the Interacting Boson Model (IBM-1). The calculated positive and negative parity energy levels showed good agreement with experimental data. The states of the first negative parity band ($K^\pi = 1^-$) are f-boson states, while the states of the second negative parity band ($K^\pi = 2^-$) are not; they may be p-boson ($L=1$) states. Theoretical calculations of electric transition probabilities $B(E1)$, $B(E2)$, and $B(E3)$ agree well with

available experimental data. The potential energy surfaces confirmed that all isotopes are deformed nuclei, mainly in a prolate shape.

Acknowledgment

The authors would like to thank the University of Basrah for their cooperation in realizing the present work.

References

- [1] A. Bohr and B. R. Mottelson, Nuclear Structure (Singapore: Word Scientific) Vol. II 748 (1998).DOI: <https://doi.org/10.1142/3530>.
- [2] G. A. Leander, W. Nazarewicz, G. F. Bertsch, J. Dudek , Low-energy collective E1 mode in nuclei, Nucl. Phys. A 453 (1986) 58-76.DOI: [https://doi.org/10.1016/0375-9474\(86\)90029-1](https://doi.org/10.1016/0375-9474(86)90029-1).
- [3] W. Nazarewicz, P. Olanders, I. Ragnarsson, J. Dudek, G. A. Leander, P. Moller, E. Ruchowsa, Analysis of octupole instability in medium-mass and heavy nuclei, Nucl. Phys. A 429 (1984) 269-295.DOI: [https://doi.org/10.1016/0375-9474\(84\)90208-2](https://doi.org/10.1016/0375-9474(84)90208-2).
- [4] W. Nazarewicz, Low energy octupole and dipole modes in nuclei, Nucl. Phys. A 520 (1990) c333-c351.DOI: [https://doi.org/10.1016/0375-9474\(90\)91158-N](https://doi.org/10.1016/0375-9474(90)91158-N).
- [5] J. F. C. Cocks, D. Hawcroft, N. Amzal, P. A. Butler, K. J. Cann, P. T. Greenlees, G. D. Jones, S. Asztalos, R. M. Clark, M. A. Deleplanque, R. M. Diamond, P. Fallon, I. Y. Lee, A.O. Macchiavelli, R.W. Macleod, F. S. Stephens, P. Jones, R. Julin, R. Broda, B. Fornal, C. T. Zhang, Spectroscopy of Rn, Ra and Th isotopes using multi-nucleon transfer reactions, Nucl. Phys. A 645 (1999) 61-91.DOI: [https://doi.org/10.1016/S0375-9474\(98\)00586-7](https://doi.org/10.1016/S0375-9474(98)00586-7).
- [6] B. M. Loc, N. Le Anh, P. Papakonstantinou, N. Auerbach, Origin of octupole deformation softness in atomic nuclei, Phys. Rev. C 108 (2023) 024303. DOI: <https://doi.org/10.1103/PhysRevC.108.024303>.
- [7] P.A. Butler, Octupole collectivity in nuclei, J. Phys. G: Nucl. Part. Phys. 43 (2016) 073002-26. DOI: <https://doi.org/10.1088/0954-3899/43/7/073002>.
- [8] K. Nomura, D. Vretenar, T. Niksic, and Bing-Nan Lu, Phys. Rev. C 89, 024312 (2014).DOI: [10.1103/PhysRevC.89.024312](https://doi.org/10.1103/PhysRevC.89.024312).
- [9] S. Cwiok and W. Nazarewicz, Reflection-asymmetric shapes in odd-A actinide nuclei, Nucl.Phys. A 529(1991) 95-114.DOI: [https://doi.org/10.1016/0375-9474\(91\)90787-7](https://doi.org/10.1016/0375-9474(91)90787-7).
- [10] P. A. Buter and W. Nazarewicz, Intrinsic dipole moments in reflection-asymmetric nuclei, Nucl. Phys. A533(1991) 249-268. DOI:[https://doi.org/10.1016/0375-9474\(91\)90489-S](https://doi.org/10.1016/0375-9474(91)90489-S).
- [11] Y. X. Liu, Y. S. Zhang, H. Z. Sun and E. G. Zhao, Pion-nucleus scattering and the spdf interacting boson model, J. Phys. G: Nucl. Part. Phys. 20 (1994) 579-592. DOI: <https://doi.org/10.1088/0954-3899/20/4/006>.
- [12] P. D. Cottle, N. V. Zamfir, Octupole states in deformed actinide nuclei with the interacting boson approximation.Phys. ReV. C 58,(1998) 1500-1514.DOI: <https://doi.org/10.1103/PhysRevC.58.1500>.
- [13] Li J., Liu Y., Gao P., SU(5) symmetry of spdfg interacting boson model, Science in China G 46 (2003) 204-2013. DOI: <https://doi.org/10.1360/03yg9028>.
- [14] M. Sugita, T. Otsuka and P von Brentano, E1 transitions in rare earth nuclei and the SPDF boson model Phys. Lett B 389 (1996) 642-648. DOI: [https://doi.org/10.1016/S0370-2693\(96\)80003-7](https://doi.org/10.1016/S0370-2693(96)80003-7).

- [15] O. Vallejos , J. Barea, Octupole and quadrupole modes in radon isotopes using the proton-neutron interacting boson model, Phys. Rev. C 104, (2021) 014308. DOI: <https://doi.org/10.1103/PhysRevC.104.014308>.
- [16] A. Arima, F. Iachello, Interacting boson model of collective states I. The vibrational limit, Ann. Phys. 99 (1976) 253-317. DOI: [https://doi.org/10.1016/0003-4916\(76\)90097-X](https://doi.org/10.1016/0003-4916(76)90097-X).
- [17] A. Arima, F. Iachello, Interacting boson model of collective nuclear states II. The rotational limit, Ann. Phys. 111, (1978) 201-238.
DOI: [https://doi.org/10.1016/0003-4916\(78\)90228-2](https://doi.org/10.1016/0003-4916(78)90228-2).
- [18] A. Arima, F. Iachello, Interacting boson model of collective nuclear states IV. The $O(6)$ limit, Ann. Phys. 123 (1979) 468-492. DOI: [https://doi.org/10.1016/0003-4916\(79\)90347-6](https://doi.org/10.1016/0003-4916(79)90347-6).
- [19] R. F. Casten, D. D. Warner, The interacting boson approximation, Rev. Mod. Phys. 60 (1988) 389-469.DOI: <https://doi.org/10.1103/RevModPhys.60.389>.
- [20] Y. X. Liu, H. Z. Sun, E. Zhao, Dynamical symmetries of the spdf interacting boson model, J. Phys. G: Nucl. Phys. 20 (1994) 407-424,DOI: <https://doi.org/10.1088/0954-3899/20/3/003>.
- [21] N. V. Zamfir, D. Kusnezov, Octupole correlations in the transitional actinides and the spdf interacting boson model, Phys. Rev. C 63 (2001) 054306-9. DOI: <https://doi.org/10.1103/PhysRevC.63.054306>.
- [22] N. V. Zamfi, D. Kusnezov, Octupole correlations in U and Pu nuclei, Phys. Rev. C 67, (2003) 014305-8,DOI: <https://doi.org/10.1103/PhysRevC.67.014305>.
- [23] K. Nomura, D. Vretenar, T. Niksic, B. N. Lu , Microscopic description of octupole shape-phase transitions in light actinide and rare-earth nuclei, Phys. Rev. C 89 (2014) 024312-16,DOI: <https://doi.org/10.1103/PhysRevC.89.024312>.
- [24] H. N. Qasim, F. H. Al-Khudair, Nuclear shape phase transition in even-even $^{158-168}\text{Hf}$ isotopes Nucl. Phys. A1002(2020)121962-17. DOI: <https://doi.org/10.1016/j.nuclphysa.2020.121962>.
- [25] K. Heyde, P. Van Isacker, M. Waroquier, J. Moreau, Triaxial shapes in the interacting boson model , Phys. Rev. C 29 (1984) 1420-1427, DOI: <https://doi.org/10.1103/PhysRevC.29.1420>.
- [26] O. Scholten, The Program Package PHINT, internal report KVI-63, Kerfysisch Versneller Instituut, Groningen, Netherlands.
- [27] ENSDF, Nuclear data Sheet (2025). Available: <http://www.nndc.bnl.gov/ensdf>.
- [28] J. Stachel, P. Van Isacker and K. Heyde, Interpretation of the $A \approx 100$ transitional region in the framework of the interacting boson mode, Phys. Rev. C 25, (1982)650-657.
DOI: <https://doi.org/10.1103/PhysRevC.25.650>.
- [29] J. N. Ginocchio, M.W. Kirson, Relationship between the Bohrcollective Hamiltonian and the interacting boson model, Phys. Rev. Lett. 44 (1980) 1744-1747. DOI: <https://doi.org/10.1103/PhysRevLett.44.1744>.

تحليل مخطط مستويات الطاقة لنظائر اليورانيوم U²³⁶⁻²²⁶ باستخدام أنموذج البوzonات المتفاولة

علي عبدالكريم مزبان* ، فالح حسين الخضير

قسم الفيزياء، كلية التربية للعلوم الصرفة، جامعة البصرة، البصرة، العراق.

معلومات البحث	الملخص
الاستلام 30 نيسان 2025	تمت دراسة التركيب النووي لنظائر اليورانيوم U ²³⁶⁻²²⁶ باستخدام أنموذج البوزنات المتفاولة (IBM-1) من أجل حساب مستويات الطاقة ذات التمايز السالب تم توسيع فضاء النموذج ليشمل البوزنون (f) ذو الزخم الزاوي (L=3). يتم وصف مستويات الحزمة الأرضية(g.s.-band) ، وحزمة بيتا(β-band) ، وحزمة غاما(γ-band) ، إضافة إلى حزمتين سالبتين التمايز. استخدمت الدوال الموجية المحسوبة لحساب احتمالات الانتقالات داخل الحزم (in-band) وبين الحزم (inter-band) . تم تحديد شكل النواة من خلال حساب سطح طاقة الجهد (PES) بدالة معاملات التشوه. تم مقارنة نتائج الأنماذج بالبيانات التجريبية المتوفرة، وأظهرت النتائج توافقًا جيدًا بشكل عام.
المراجعة 24 أيار 2025	
القبول 26 أيار 2025	
النشر 30 حزيران 2025	

الكلمات المفتاحية

مستويات الطاقة، التركيب النووي،
أنموذج البوزنات المتفاولة ،
الأنوية الثقيلة، نظائر اليورانيوم.

Citation: A. A. Mezban , F. H. Al-Khudair, J.Basrah Res. (Sci.) 51(1),159 (2025).
DOI:<https://doi.org/10.56714/bjrs.51.1.14>

*Corresponding author email: pgs.ali.abdalkareem@uobasrah.edu.iq



©2022 College of Education for Pure Science, University of Basrah. This is an Open Access Article Under the CC by License the [CC BY 4.0](#) license.

N: 1817-2695 (Print); 2411-524X (Online)
line at: <https://jou.jobrs.edu.iq>